Available online at www.sciencedirect.com
SCIENCE DIRECT®
Journal of Organometallic Chemistry 668 (2003) 9–16
Journal of Organometallic Chemistry
www.elsevier.com/locate/jorganchem

Redox activation of dicarbonyl(η^5-cyclopentadienyl)methyl iron within the cavity of β-cyclodextrin: carbon monoxide insertion in iron–methyl bond

Lubomír Pospíšil [a,*], Magdaléna Hromadová [a], Jan Fiedler [a], Christian Amatore [b], Jean-Noël Verpeaux [b]

[a] *J. Heyrovský Institute of Physical Chemistry, Czech Academy of Sciences, Prague, Czech Republic*
[b] *Ecole Normale Superieure, UMR 8640 'PASTEUR', 24, rue Lhomond, 75231 Paris Cedex 05, France*

Received 29 July 2002; accepted 26 November 2002

Abstract

The organometallic complex $CpFe(CO)_2CH_3$ is included in a β-cyclodextrin cavity, retains its redox activity and undergoes CO insertion into the methyl–metal bond. The reaction inside the cavity suppresses undesirable loss of released CO from the reaction site. This simplifies the mechanism of the bond-insertion reaction in the presence of cyclodextrin. Further enhancement is observed in presence of free CO, which can penetrate to the reaction site inside the cyclodextrin cavity.

Keywords: Redox activation; Beta-cyclodextrin; Host–guest complex; CO insertion; Dicarbonyl(η5-cyclopentadienyl)methyl iron

1. Introduction

Cyclodextrins are capable of including a variety of organic and inorganic guests within their hydrophobic cavities. While the inclusion of organic molecules is documented in a large number of publications, much less attention has been paid to inclusion of organometallic compounds. In all instances, the protecting influence of the cyclodextrin cavity to electron transfer reaction pathways has been rarely considered. The first organometallic inclusion complexes with cyclodextrins were prepared from ferrocene and its derivatives [1–5]. Later, the cyclodextrin encapsulation of various metal carbonyl complexes has been described [6–8]. Of particular importance for this study is a report confirming host–guest complexation of dicarbonyl(η^5-cyclopentadienyl)alkyl iron [9,10]. It was shown that an iron complex inside the β-cyclodextrin (βCD) cavity inserts CO in the iron–alkyl bond in the solid state at elevated temperature. Our previous electrochemical study of dicarbonyl(η^5-cyclopentadienyl)methyl iron, **1**, showed that redox activation of the coordination sphere triggers the same carbonylation reaction, however, it proceeds catalytically at ambient temperature and pressure [11]. The catalytic cycle is achieved by a homogeneous reaction of electrogenerated radical anion of acyl derivative of iron (**2**) and the parent complex. Ligand substitution by solvent and acyl migration onto the Cp ring were identified as principal terminations steps of the catalytic process, though the former serves at the same time as a source of additional free CO, participating in the catalytic cycle. The compounds participating in the overall process are given in Scheme 1.

In this communication, we report an attempt to eliminate termination reactions by performing the redox activation within the protecting environment created by the cyclodextrin cavity. Termination reactions could then be eliminated or at least substantially suppressed.

* Corresponding author.
E-mail address: pospisil@jh-inst.cas.cz (L. Pospíšil).

0022-328X/02/$ - see front matter
doi:10.1016/S0022-328X(02)02142-3

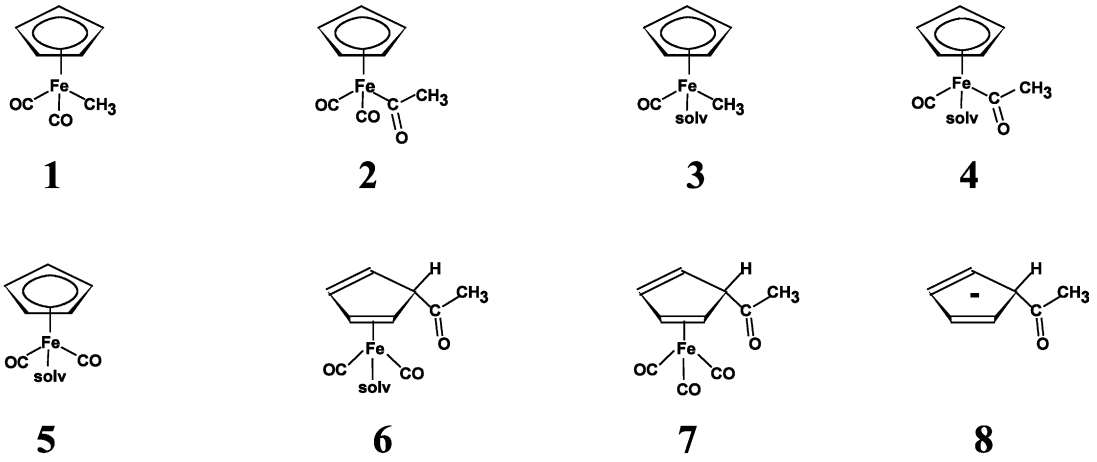

Scheme 1.

2. Experimental

Measurements were done using a home-built electrochemical system for cyclic voltammetry and dc polarography based on a fast rise-time potentiostat [12]. The instruments were interfaced to a personal computer via an IEEE-interface card (PC-Lab, AdvanTech Model PCL-848) and a data acquisition card (PCL-818) using 12-bit precision. A three-electrode electrochemical cell was used. The reference electrode, Ag|AgCl|1 M LiCl, was separated from the test solution by a salt bridge, and the half-wave potential of ferrocene against it was +0.562 V. The working electrode was a valve-operated static mercury electrode (SMDE2, Laboratorní Přístroje, Prague) with an area 1.13×10^{-2} cm^2. The auxiliary electrode was cylindrical platinum net. The exhaustive electrolysis was performed using the mercury pool electrode with 1.9 cm^2 area. The potential control and the faradaic charge measurements were done using Potentiostat/Galvanostat P.A.R., model 263 (EG&G Princeton Applied Research, USA). In difference with standard procedures, here the potential for electrolysis was set at the onset of the faradaic current. The charge corresponding to uptake of one electron per molecule was allowed to pass and voltammograms were immediately taken. Oxygen was removed from the solution by passing a stream of argon through it. Argon and carbon monoxide were purchased in the highest purity grade from Linde. Carbon monoxide was purified from volatile pentacarbonyl iron by a procedure described before [13]. Tetrabutylammonium hexafluorophosphate (Aldrich), used as the supporting electrolyte, was recrystallized and vacuum-dried. Anhydrous dimethylsulfoxide (99.9% A.C.S. spectrophotometric grade with water content $< 0.01\%$) was obtained from Aldrich and was used as received. Inclusion complexes of two organometallic compounds, $CpFe(CO)_2CH_3$ (**1**) and $CpFe(CO)_2(COCH_3)$ (**2**), and βCD were prepared according to published procedure [9] by precipitation from suspensions of the corresponding compound in aqueous βCD solution. Equimolar suspensions were mixed 1 day at temperature 45 °C. The resulting pale yellow precipitate was filtered and uncomplexed reactants were washed away by water and subsequently by dichloromethane. The ^{1}H-NMR (d^6-Me_2SO) spectrum of [**1**·βCD] was identical with previously published data [10]. Voltammetric anodic peak potentials were assigned to corresponding reaction products on the basis of identification performed previously by means of preparative electrolysis, GC/MS and in situ FTIR [11].

3. Results

3.1. Reduction of 1 (FpMe) in DMSO

Our previous report describes in detail the mechanism of reduction of **1** in which the redox activated homogeneous reaction and several termination steps were identified. We found that solvent substitution reactions play an important role in acetone, however, other solvents also readily substitute ligands of **1** in its labile reduced form. Non-polar solvents do not dissolve cyclodextrin complexes and hence it was necessary to perform the present study under rather different conditions. Present measurements were done in DMSO, which is an excellent solvent for cyclodextrins and their complexes. However, the solubility of cyclodextrins and miscibility of DMSO with other solvents imposes sever separation problems to identify small amounts of final products along a surplus of the indifferent electrolyte. This lead us to an approach in which resulting products and intermediates would be identified on basis of electrochemical characteristics assigned to corresponding derivatives in our previous study [11]. In order to verify the feasibility of this approach, we investigated possible differences in redox chemistry of **1** when DMSO is used. We recorded a series of voltammograms

of **1** in DMSO at various scan rates and accumulation potentials. Voltammograms were taken both under an inert atmosphere of Ar and in samples saturated with gaseous CO. Figs. 1 and 2 summarize relevant observations. The irreversible reduction at the peak potential −2.03 V yielded five more or less intensive anodic peaks of products at −0.3 ($\mathbf{7}^{\bullet -}$), −0.57 ($\mathbf{6}^{\bullet -}$), −0.88 ($\mathbf{5}^{-}$), −1.07 ($\mathbf{4}^{\bullet -}$) and −1.37 V ($\mathbf{3}^{\bullet -}$), respectively. Since all the anodic peak potentials in DMSO matched reasonably with those found previously [11] the assignment of five peaks in Fig. 1 to [(η_4-Cp(H)Acyl)Fe(CO)$_3$] ($\mathbf{7}^{\bullet -}$), [(η_4-Cp(H)Acyl)Fe(CO)$_2$·Solv] ($\mathbf{6}^{\bullet -}$), [CpFe(CO)$_2$·Solv] ($\mathbf{5}^{-}$), [CpFe(CO)(Acyl)·Solv] ($\mathbf{4}^{\bullet -}$) and [CpFe(CO)CH$_3$·Solv] ($\mathbf{3}^{\bullet -}$), where Solv is the coordinated solvent, is valid also in DMSO. The assignment is substantiated by the following experimental observations. The presence of free CO suppressed the formation of all products except $\mathbf{7}^{\bullet -}$ observed as a peak at −0.3 V (Fig. 2). The two most negative anodic peaks showed electrochemical reversibility at the scan rate 61 V s^{-1}. At this scan rate the presence of free CO revealed the existence of still another transient product oxidized at −1.52 V. The transient redox pair at $E_{1/2} = -1.37$ V was eliminated by a high scan rate, while the transient redox pair at $E_{1/2} = -1.10$ V was enhanced. These

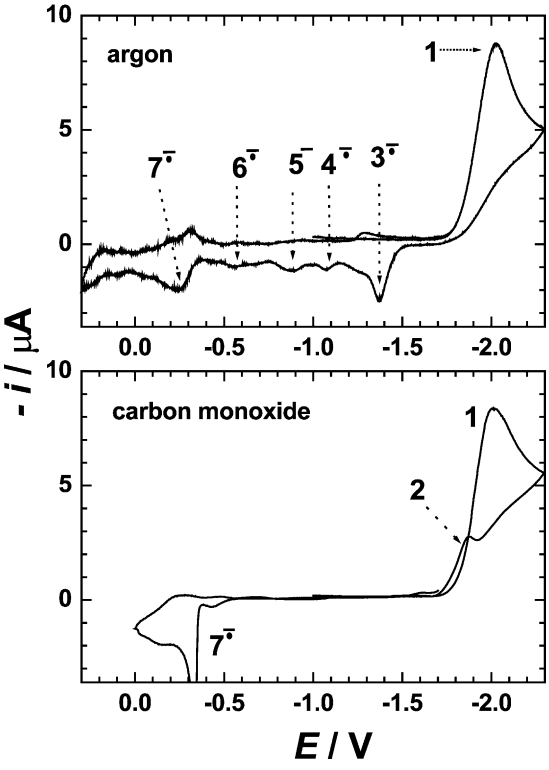

Fig. 1. Cyclic voltammetry of 1 mM CpFe(CO)$_2$CH$_3$ (**1**) in 0.1 M tetrabutylammonium hexafluorophosphate in DMSO at a static mercury drop electrode (area 1.13×10^{-2} cm^{-2}). Curves were recorded under an argon atmosphere or in samples saturated with carbon monoxide. The scan rate was 0.5 V s^{-1}. Numbers refer to compounds given in Scheme 1.

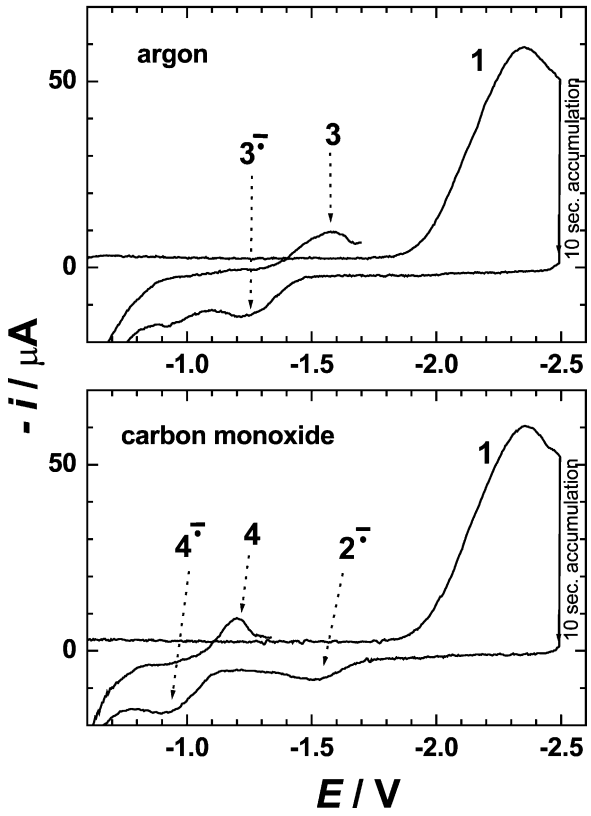

Fig. 2. Fast cyclic voltammetry (61 V s^{-1}) of 1 mM CpFe(CO)$_2$CH$_3$ (**1**) in 0.1 M tetrabutylammonium hexafluorophosphate in DMSO at a static mercury drop electrode (area 1.13×10^{-2} cm^{-2}). Curves were recorded under an argon atmosphere or in samples saturated with carbon monoxide. The polarization voltage was held at the vertex potential −2.5 V for 10 s. Numbers refer to compounds given in Scheme 1.

finding leads us to the conclusion that in DMSO the reaction mechanism is the same as previously described (Scheme 2).

We want to stress that the presence of free CO does not increase the intensity of the main reduction peak at −2.03 V in all the experiments just described. We will refer to this important feature in the forthcoming paragraphs.

3.2. Reduction of inclusion complex [*1*·βCD] in DMSO

Voltammetry of [**1**·βCD] under the same conditions as described in the previous section is given in Fig. 3. It shows a marked difference of electron transfer mechanism caused by the protecting environment of the cyclodextrin cavity. The main reduction peak at −2.03 V is located at the same potential as the reduction of free **1**, however, its height is smaller by 13%. Such a small current value is in accordance with a smaller diffusion coefficient (ca. by 20%) of the host–guest complex. More striking is the fact that the number of anodic peaks of reaction products has diminished to show only two peaks at −0.97 and −0.7 V corresponding most

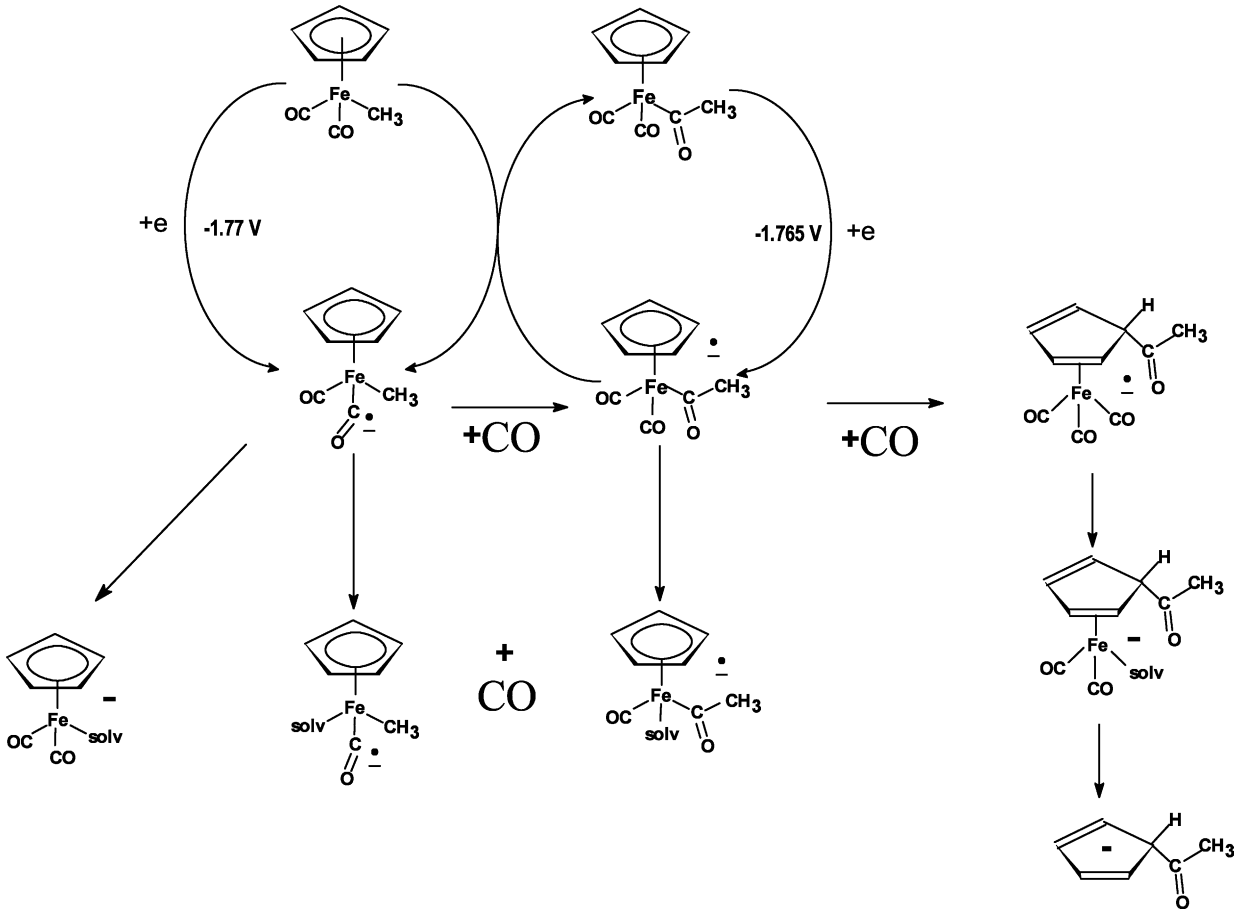

Scheme 2.

likely to complexed forms of $\mathbf{4}^{\bullet -}$ and $\mathbf{5}^{-}$, respectively. The assignment of $\mathbf{5}^{-}$ is further discussed below. Voltammetry performed in samples saturated with gaseous carbon monoxide yielded another striking difference between redox properties of the free and complexed **1**. The reduction peak current at -2.03 V in the presence of free CO was considerably higher than under the argon atmosphere. A similar increase of the diffusion-limited reduction current was observed also in *dc* polarograms. The half-wave potential and the transfer coefficient α in both cases have identical values of -1.92 and 0.42 V, respectively. We note that such a current increase was not observed for the free form **1** (Fig. 1). The kinetic effect of the free CO is confirmed by fast voltammetry (Fig. 4). At a scan rate of 61 V s^{-1} the reduction peak has the same height regardless of the presence of argon or carbon monoxide. Furthermore, by replacing argon with CO, one can see the disappearance of the side-product $[\mathbf{4}\cdot\beta CD]^{\bullet -}$ (anodic peak at -1.07 V) and a remarkable increase of $\mathbf{2}^{\bullet -}$ formation, seen as a reversible redox pair of peaks at $E_{1/2} = -1.75$ V. In a fast experiment, the shorter time constant eliminates the formation of an essential intermediate responsible for higher rate of consumption of $[\mathbf{1}\cdot\beta CD]$, however, it allows the observation of highly reactive species. In the present case, it is the freezing at the scan rate 61 V s^{-1} of the reaction between **1** and $\mathbf{2}^{\bullet -}$ which allows the observation of the anodic and cathodic redox peaks of the couple $\mathbf{2/2}^{\bullet -}$. The assignment of an anodic peak at -0.7 V to the product $\mathbf{5}^{-}$ is based on the observation that this peak is found only in the presence of βCD for both **1** and **2**. The excess of carbon monoxide eliminates this peak. The wave at -0.7 V is less intense for $[\mathbf{1}\cdot\beta CD]$ than for $[\mathbf{2}\cdot\beta CD]$, which suggests again that it features solvent substituted $CpFe(CO)_2\cdot Solv$ formed by a replacement of the acyl ligand. Indeed upon starting with **1**, compound $\mathbf{2}^{\bullet -}$ is formed from $\mathbf{1}^{\bullet -}$, however, this anion radical participates in a homogeneous reaction with **1** which decreases the yield of $\mathbf{5}^{-}$. This competitive step does not occur during the reduction of authentic $[\mathbf{2}\cdot\beta CD]$ in the absence of **1**. The species $\mathbf{5}^{-}$ could be formed by methyl abstraction from $\mathbf{1}^{\bullet -}$, as was pointed by the referee. We do not consider it likely because the corresponding anodic peak at -0.7 V is not observed in the reduction of the free **1** (Fig. 1).

The inherent reactivity of derivatives yielding anodic peaks thus described suggests that these compounds may not be the final stable products. In order to estimate the distribution of final products under the protecting environment of βCD cavity we compared the

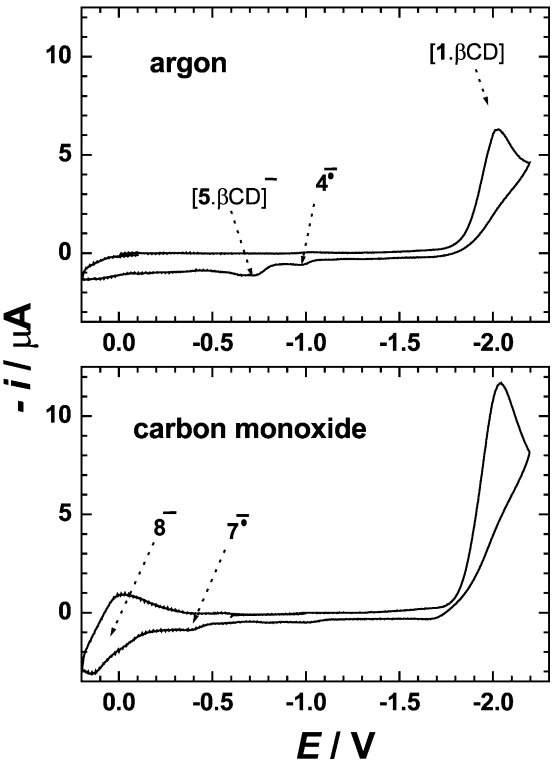

Fig. 3. Cyclic voltammetry of 1 mM $[CpFe(CO)_2CH_3 \cdot \beta CD]$ ($[\mathbf{1} \cdot \beta CD]$) in 0.1 M tetrabutylammonium hexafluorophosphate in DMSO at a static mercury drop electrode (area 1.13×10^{-2} cm^{-2}). Curves were recorded under an argon atmosphere or in samples saturated with carbon monoxide. The scan rate was 0.5 V s^{-1}. Numbers refer to compounds given in Scheme 1.

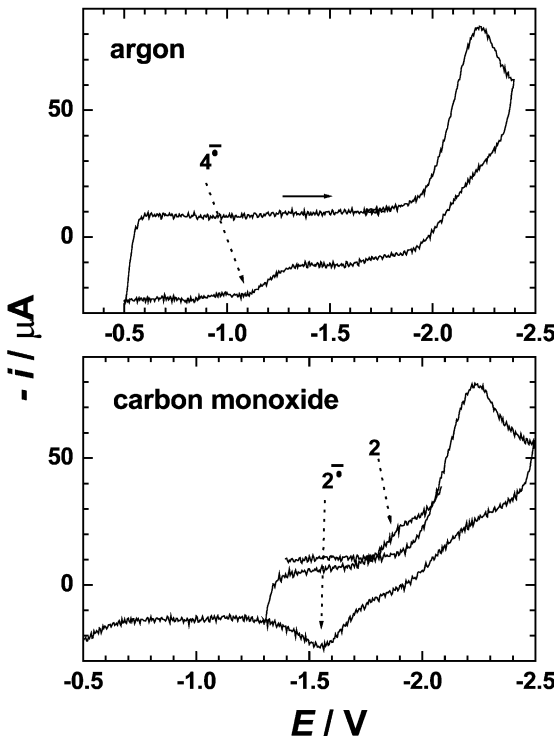

Fig. 4. Fast cyclic voltammetry (61 V s^{-1}) of 1 mM $[CpFe(CO)_2CH_3 \cdot \beta CD]$ ($[\mathbf{1} \cdot \beta CD]$) in 0.1 M tetrabutylammonium hexafluorophosphate in DMSO at a static mercury drop electrode (area 1.13×10^{-2} cm^{-2}). Curves were recorded under an argon atmosphere or in samples saturated with carbon monoxide. The initial potential was −0.5 V.

pattern of redox peaks observed after the preparative electrolysis of free **1** and $[\mathbf{1} \cdot \beta CD]$. Indeed, the electrolysis of $[\mathbf{1} \cdot \beta CD]$ yields almost fourfold increase in total yield of **2** and a substantial suppression of formation of compounds **5**–**7**.

3.3. Reduction of 2 in DMSO

The acyl derivative $\mathbf{2}^{\bullet -}$ formed from $\mathbf{1}^{\bullet -}$ by the insertion reaction of coordinated CO to the iron–methyl bond and by subsequent homogeneous electron transfer with unreacted **1** has the key role in the catalytic process [11]. Hence, a meticulous inspection of its properties in the free form and in the inclusion complex is important for assessment of the mechanism of cavity-confined reactions. Selected relevant voltammograms of an authentic sample of **2** are given in Fig. 5. These voltammograms provide evidence that the product $\mathbf{4}^{\bullet -}$ featured by the redox couple at $E_{1/2} = -1.07$ V, observed in previous figures relative to **1**, indirectly originates from the reduction of **2**. This follows from the comparison of Fig. 5A and B. When the potential scan was paused at −2.2 V, an increased production of $\mathbf{4}^{\bullet -}$ at the expense of $\mathbf{2}^{\bullet -}$ was observed (Fig. 5B). Hence, this confirmed that the redox process at −1.07 V is due to the solvent substituted redox pair $\mathbf{4/4}^{\bullet -}$. The saturation of solution with gaseous CO eliminated the detection of $\mathbf{2}^{\bullet -}$ at a slow scan rate 0.5 V s^{-1} (Fig. 5C). The presence of an excess of free CO in the solution makes $\mathbf{2}^{\bullet -}$ more unstable, which results in the disappearance of the anodic peak of $\mathbf{2}^{\bullet -}$. A modification of the reduction scheme including further evolution of $\mathbf{2}^{\bullet -}$ also follows from a 30% increase of the main reduction peak at −1.8 V (compare Fig. 5A and C). Even at the scan rate of 61 V s^{-1} the presence of free CO influenced the height of the anodic branch of the voltammetric curve (Fig. 5D). This is in agreement with our previous study in acetone [11], where the instability of $\mathbf{2}^{\bullet -}$ was documented. Electrochemical activation of **2** causes an enhanced rate of acyl migration from the metal center to Cp ligand and hence a facile substitution. This can be seen as the growth of the anodic peak of product containing the acyl group. The anodic peak, observed at −0.37 V ($\mathbf{7}^{\bullet -}$), corresponds to a derivative formed by acyl migration $[(\eta_4\text{-Cp(H)Acyl})Fe(CO)_3]$. We can conclude that the solvent substitution reactions of ligands of $\mathbf{2}^{\bullet -}$ are more pronounced in DMSO than in other solvents used previously.

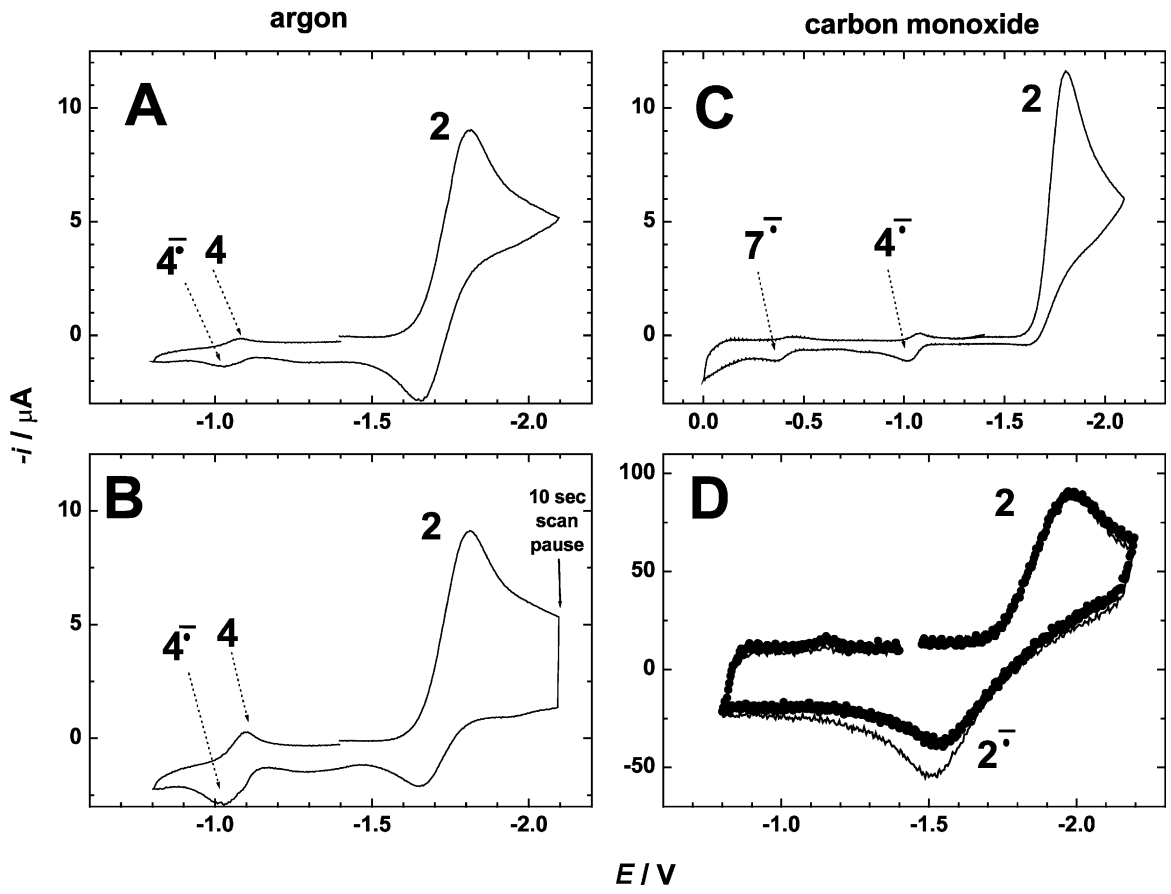

Fig. 5. Cyclic voltammetry of 1 mM $CpFe(CO)_2(COCH_3)$ (**2**) in 0.1 M tetrabutylammonium hexafluorophosphate in DMSO at a static mercury drop electrode (area 1.13×10^{-2} cm^{-2}). Curves in (A) and (B) were recorded under an argon atmosphere, curves in (C) were measured in sample saturated with gaseous CO. The scan rate was 0.5 V s^{-1}. Curve in (A) was obtained with a triangular voltage–time waveform. The curve in (B) was measured with a trapezoidal voltage–time function performing the product accumulation for 10 s at −2.2 V. Curves in (D) give voltammograms at 61 V s^{-1} in argon (full line) and in the presence of CO (full points).

3.4. Reduction of inclusion complex [2·βCD] in DMSO

Voltammetry in samples prepared from a solid complex [**2**·βCD] yielded a different picture than free **2** (Fig. 6). The main reduction peak was located at the same potential −1.8 V, however, it was smaller and less reversible. Furthermore, scanning the potential to −2.2 V showed the presence of a second redox couple at −2.0 V. The anodic peaks of products were located at −1.04, −0.72 and near 0 V. Peaks at −0.72 and −0.05 V intensified, when the potential scan was reversed at −2.2 V. These observations lead to the conclusion that [**2**·βCD] undergoes the dissociation equilibrium. Such a dissociation yields the free **2** (peak potential at −1.8 V), whereas the complex is reduced at peak potential −2.0 V. The formation of the complexed form [**2**·βCD] in DMSO was confirmed by stepwise addition of a surplus of βCD to a solution of **2**, which yielded a progressive increase of the identical peak at −2.0 V and a concomitant decrease of the peak at −1.8 V. Since the inclusion of a guest in to the CD cavity involves

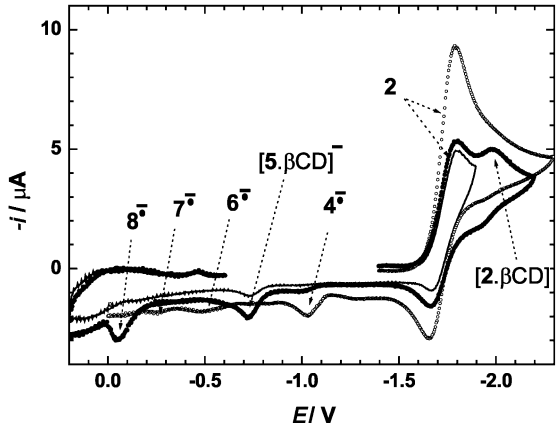

Fig. 6. Cyclic voltammetry of 1 mM $[CpFe(CO)_2(COCH_3)\cdot\beta CD]$ ([**2**·βCD]) (line and full points) or uncomplexed **2** (opened points) in 0.1 M tetrabutylammonium hexafluorophosphate in DMSO at a static mercury drop electrode (area 1.13×10^{-2} cm^{-2}). The scan rate and the initial potential were 0.5 V s^{-1} and −0.8 V, respectively.

expulsion of the cavity-bound solvent, the formation of [**2**·βCD] in DMSO is less favorable than in water

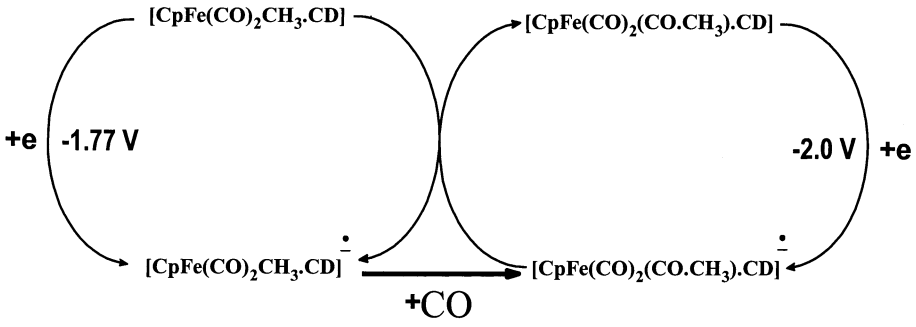

Scheme 3.

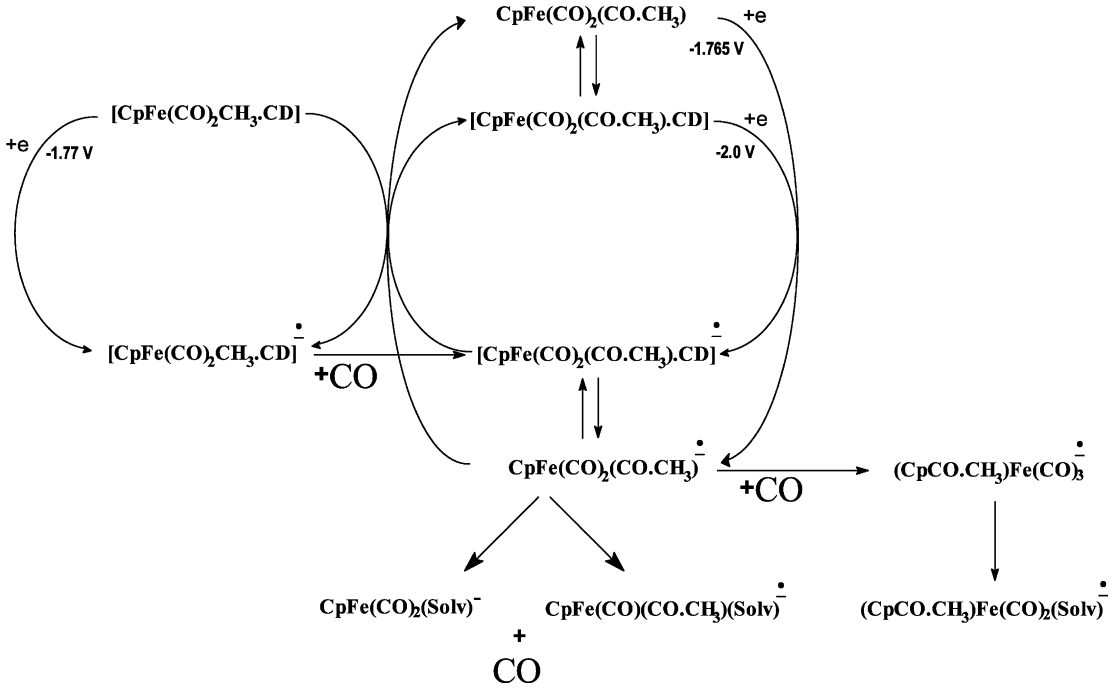

Scheme 4.

where solid [**2**·βCD] was prepared. This is in accordance with well-known experience that inclusion complexes can be prepared only in aqueous medium [14].

An excess of free CO increases the amount of product $\mathbf{8}^-$ oxidized near 0 V and makes the wave at −0.37 V more distinct. Other products are suppressed by the presence of free CO in the solution. The anodic peak at −0.72 V is observed in voltammograms of both **1** and **2**, but only when βCD is present, and this wave is eliminated in the presence of CO. This characteristic suggests that the corresponding product were formed by solvent substitution of the acyl ligand inside the cavity where DMSO is also included. Since $\mathbf{2}^{\bullet -}$ formed from $\mathbf{1}^{\bullet -}$ participates in the reduction cycle, the transformation $\mathbf{2}^{\bullet -} \rightarrow \mathbf{5}^-$ is less efficient on voltammograms of [**1**·βCD] than on curves obtained for [**2**·βCD]. This can be seen by comparison of Fig. 3 and Fig. 6.

4. Discussion

The results described in the preceding section undoubtedly show a rather profound change of the overall reaction mechanism of the reduction of **1** when included in the supramolecular complex [**1**·βCD]. One effect of the nano-environment of the cyclodextrin cavity is the elimination of some of the side-reactions as seen by the disappearance of certain anodic peaks of intermediates and/or products. Another remarkable feature is a pronounced increase of the reduction current in an atmosphere of CO. Data obtained for the inclusion complex of **2** indicate that the key intermediate [**2**·βCD]$^{\bullet -}$ can be included in the cyclodextrin cavity. Therefore, it is evident that in the reduction of [**1**·βCD] the following overall homogeneous cross-reaction participates

$$[\mathbf{1}\cdot\beta CD] + [\mathbf{2}^{\bullet -}\cdot\beta CD] \overset{^1k_f}{\rightarrow} [\mathbf{1}^{\bullet -}\cdot\beta CD] + [\mathbf{2}\cdot\beta CD] \quad (1)$$

Due to the close proximity of redox potentials of both $[\mathbf{1}\cdot\beta CD]$ and $[\mathbf{2}\cdot\beta CD]$, the reaction sequence contains a cyclic regeneration of $[\mathbf{2}\cdot\beta CD]^{\bullet -}$, as is shown in Scheme 3.

Scheme 3 gives the primary heterogeneous redox activation step as the leftmost reaction proceeding at −1.77 V. The homogeneous cross-reaction in the vicinity of the electrode surface is symbolized by two arrows in the middle of Scheme 3, whereas the heterogeneous redox regeneration of the reactant $\mathbf{2}^{\bullet -}$ is the rightmost reaction in Scheme 3. Further processes to be considered include the dissociation equilibria and inherent instability of $\mathbf{2}^{\bullet -}$ in the presence of free CO. The detailed mechanism is rather complicated and still not fully elucidated. Nevertheless, the redox characteristics at different time scales presented here are consistent with the reaction mechanism given in Scheme 4.

Side-reactions presented by anodic peaks of $\mathbf{4}^{\bullet -}$, $\mathbf{5}^{-}$, $\mathbf{7}^{\bullet -}$ and $\mathbf{8}^{\bullet -}$ (Fig. 3) originate not from $[\mathbf{1}\cdot\beta CD]^{\bullet -}$ but from free $\mathbf{2}^{\bullet -}$ released due to the dissociation equilibrium.

At this stage of investigations, attempts to elucidate quantitatively the protecting effect of cyclodextrin cavity on the stability of intermediates by numerical simulation techniques are still hampered by a large number of chemical steps and corresponding parameters. All voltammograms presented in previous sections show different degrees of coupling heterogeneous charge transfer reactions and subsequent chemical reactions of reactive intermediates that generate electroactive products. Preliminary simulation results indicate close proximity of standard redox potentials of couples $\mathbf{1}/\mathbf{1}^{\bullet -}$ and $\mathbf{2}/\mathbf{2}^{\bullet -}$ and the standard heterogeneous constants k^0 values 3×10^{-4} and 3×10^{-3} cm s^{-1}, respectively. The remarkable effect of the cyclodextrin causing a higher overall production of **2**, is caused by a nanometric confinement preventing that an essential reactant, the free CO released by ligand substitution reactions, diffuses from the reaction site.

Acknowledgements

This work was financially supported by the Ministry of Education of the Czech Republic within the COST program (OCD15.10), the Grant Agency of the Czech Rep. (203/02/P082) as well as by CNRS (UMR 8640), ENS and MRT.

References

[1] T. Matsue, D.H. Evans, T. Osa, N. Kobayashi, J. Am. Chem. Soc. 107 (1985) 3411.
[2] A. Harada, Y. Hu, S. Yamamotom, S. Takahashi, J. Chem. Soc. Dalton Trans. (1988) 729.
[3] A.D. Ryabov, E.M. Tyapochin, S.D. Varfolomeev, A.A. Karyakin, Biochem. Bioenerg. 24 (1990) 257.
[4] V.V. Strelets, I.A. Mamedjarova, M.N. Nefedova, N.I. Pysnograeva, V.I. Sokolov, L. Pospíšil, J. Hanzlík, J. Electroanal. Chem. 310 (1991) 179.
[5] W. Kutner, K. Doblhofer, J. Electroanal. Chem. 326 (1992) 139.
[6] A. Harada, K. Saeki, S. Takahashi, Organometallics 8 (1989) 730.
[7] M. Shimada, Y. Morimoto, S. Takahashi, J. Organometal. Chem. 443 (1993) C8.
[8] L. Song, Q. Meng, X. You, J. Organometal. Chem. 498 (1995) C1.
[9] M. Shimada, A. Harada, S. Takahashi, J. Chem. Soc. Chem. Commun. (1991) 263.
[10] P.P. Patel, M.E. Welker, J. Organometal. Chem. 547 (1997) 103.
[11] C. Amatore, M. Bayachou, J.-N. Verpeaux, L. Pospíšil, J. Fiedler, J. Electroanal. Chem. 387 (1995) 101.
[12] L. Pospíšil, J. Fiedler, N. Fanelli, Rev. Sci. Instrum. 71 (2000) 1804.
[13] J. Fiedler, M. Salmain, G. Jaouen, L. Pospíšil, Inorg. Chem. Commun. 4 (2001) 613.
[14] J. Szejtli, Cyclodextrins and Their Inclusion Complexes, Akademiai Kiado, Budapest, 1982, p. 102.